Thermodynamic Properties of Supercooled Fe-B Liquids—A Theoretical and Experimental Study

O. Tolochko and J. Ågren

(Submitted 22 December 1998; in revised form 31 October 1999)

The two-level model, recommended at the Ringberg 95 workshop, is applied to extrapolate the thermodynamic properties of liquid Fe-B alloys to large undercooling and to analyze the crystallization of glassy $Fe_{85}B_{15}$ alloys obtained by melt spinning. The new method yields practically the same phase diagram as the SGTE database but a superior result when evaluating the heat capacity, entropy, and crystallization heat at large undercooling. These properties are compared in the low-temperature range (700 to 800 K) with the experimental data obtained for an $Fe_{85}B_{15}$ metallic glass by scanning calorimetry. A good agreement between experiments and calculations is obtained when the observed magnetic transition at 530 K is taken into account.

1. Introduction

It is common to approximate the driving force for crystallization as proportional to the undercooling. As the undercooling increases, this approximation becomes less reliable because the real driving force is lower than that predicted from proportionality. This behavior has been discussed by many authors, and several mathematical expressions have been suggested on a more or less ad hoc basis, see, for example, the work by Lele *et al.* [1985Lel]. The main reason for the nonlinear behavior is the structural changes of the liquid upon cooling, whereby the entropy of the liquid decreases faster than that of the crystalline phase. These changes are revealed in a pronounced increase of the heat capacity of a liquid upon cooling. Provided that crystallization can be avoided, the structural changes continue until there is a glass transition below which the structure freezes due to sluggish kinetics. If such a glass is heat treated below the glass transition, there may be time for further structural changes, whereby the liquid would approach a state of internal equilibrium. The difference in Gibbs energy between the nonequilibrium glass and the undercooled liquid in internal equilibrium yields the driving force for structural relaxation.

Moreover, the Gibbs energy of the liquid is needed when calculating phase diagrams using the CALPHAD method. The early calculations were based on Gibbs energy expressions with linear temperature dependencies, whereas later ones also included the heat capacities yielding terms of the type $-c$ ln T. The inclusion of the heat capacity improves the thermodynamic description in the temperature range where the value of the heat capacity is well established but may lead to less satisfactory results upon extrapolations. For example, a constant heat capacity difference between liquid and crystalline phase may yield the unphysical prediction that the crystal would melt if the temperature is low enough. This may cause problems when calculating phase diagrams with large differences in melting point between the constituents. In order to avoid this problem, Dinsdale *et al.* [1991Din] have suggested extrapolation of C_P^L and C_P^S, respectively, in such a way that the difference between these goes to zero approximately at 0.5 and 1.5 T_m, respectively. This method ensures that the Gibbs energy curves intersect only once, *i.e.*, at the melting point. However, the resulting behavior of the C_P function becomes rather artificial.

Ågren [1988Agr] suggested a more physically based model of representing thermodynamic properties of liquids. The model is based on the assumption that the constituents may be in a solid- or liquidlike state. Recently, the Ringberg 95 workshop recommended this model for representing thermodynamic properties of liquids [1995Agr]. The model was successfully used for the pure metals such as Sn [1988Agr, 1995Agr] and Cu [1995Agr] as well as nonmetallic SiO_2 and glycerol [1988Agr].

In general, it is difficult to study experimentally the properties of highly undercooled liquid metals because the crystallization is very rapid. However, valuable information may be obtained from the properties of rapidly quenched amorphous metallic materials. There are several reasons for this.

- Glass formation in metallic systems occurs at an undercooling of several hundred degrees below the melting point.
- Metallic glasses have an extremely wide range for the glass transition compared with traditional glasses such as oxides and polymers.
- Metallic glasses are highly unstable causing secondary structural relaxation processes occurring at temperatures considerably below the glass transition interval [1991Tol].

The purpose of the present paper is to analyze the properties of the binary Fe-B system and obtain a description of the supercooled liquid based on the two-level model [1988Agr, 1995Agr]. In the concentration range of glass forming, the

O. Tolochko, Material Science Faculty, State Technical University, 195251 Saint-Petersburg, Russia; and **J. Ågren,** Department of Materials Science and Engineering, Royal Institute of Technology, S-100 44 Stockholm, Sweden.

results will be compared with the low-temperature experimental data, enthalpy differences between metastable liquid, and stable crystalline state and heat capacity of liquid obtained by differential scanning calorimetry (DSC) for Fe-B metallic glasses.

2. Experimental Procedure

The specimen used in the present work was an Fe-base alloy containing 15 at. % B. Mixtures of pure metals and metalloids were melted under an argon protective atmosphere in an induction furnace. Continuous ribbon-shaped specimens close to 40 μ thick and 10 mm wide were prepared by melt spinning using a copper disk with a diameter 300 mm. After quenching, the alloy was x-ray amorphous. Later, transmission electron microscope (TEM) investigations confirmed that the alloy was amorphous.

Heat effects of crystallization and heat capacity values were measured on a DSM-2M scanning calorimeter upon heating at a rate 16 K/min. X-ray diffraction experiments were carried out by a DRON-3.0 diffractometer (Fe K_α monochromatic radiation) and a Philips diffractometer "PW3710 BASED" (Cu K_α radiation) (Philips Electronic Instruments Corp., Mahwah, NJ). Microstructure of the specimens after annealing was investigated using a JEOL 2000-EX transmission electron microscope (TEM) (Japan Electron Optics Ltd., Tokyo).

3. Model Calculations

The two-state model [1988Agr, 1995Agr] yields the following expression for the Gibbs energy of the liquid G_m^L:

$$G_m^L = G_m^{sol} - RT\ln\left[1+\exp\left(-\ddot{A}G_d/RT\right)\right] \qquad \text{(Eq 1)}$$

where R is the gas constant, T is the temperature, and $\Delta G_d = {}^0G_m^{liq} - {}^0G_m^{sol}$, where ${}^0G_m^{liq}$ and ${}^0G_m^{sol}$ are the molar Gibbs energy for the hypothetical cases with all the atoms in the liquid- and solidlike states, respectively.

For Fe and B, the experimental information is not extensive enough to reveal any temperature dependence of heat capacity in the liquid state c_p^{liq}. For B, only a single value at the melting point is available. For Fe, we used several groups of experimental data in the temperature interval 1811 to 2000 K. In Ref [1995Agr], it was shown that it is reasonable to base the quantity ${}^0G_m^{sol}$ on the Gibbs energy of a stable crystalline state. In the present analysis, we have chosen the following expression:

$${}^oG_m^{sol}(Fe) = {}^oG_{Fe}^{fcc} + A + BT\ln T + DT^2 - RT \qquad \text{(Eq 2)}$$

for Fe and

$${}^oG_m^{sol}(B) = {}^oG_B^{beta} + A' + B'T\ln T + D'T^2 - RT \qquad \text{(Eq 3)}$$

for B, where ${}^0G_{Fe}^{fcc}$ and ${}^0G_B^{beta}$ are the Gibbs energies of the stable fcc Fe and β-B phases, respectively. For ΔG_d, we rather arbitrarily take

$$\Delta G_d = \Delta H_{melting} - RT \qquad \text{(Eq 4)}$$

where $\Delta H_{melting}$ is equilibrium crystallization enthalpy.

For each element, there are three parameters *A, B,* and *D,* which have been optimized using the experimental information on the equilibrium melting point $T_{melting}$, $\Delta H_{melting}$, and c_p^{liq} in the neighborhood of the melting point. For all calculations, the Thermo-Calc [1985Sun] system was used.

3.1 New Description of Liquid Fe

The optimization was performed adjusting to the information presented in Table 1. Determination of optimum values of the parameters was based on nonlinear least-squares fit to the experimental points. The following parameters were obtained:

$$A = 6,579.16 + H_{Fe}^{SER}\ \text{J mol}^{-1},\ B = -0.0013\ \text{J mol}^{-1}\ \text{K}^{-2},$$
$$D = 1.75\ \text{J mol}^{-1}\ \text{K}^{-1}$$

The term "SER" denotes the so-called "stable element reference," *i.e.*, the element in its stable state at 298.15 K. In Table 1, we have also presented the values calculated from the new description. The entropies of the liquid, fcc, and bcc phases in pure Fe are shown in Fig. 1.

3.2 New Description of Liquid B

The optimization of parameters was performed adjusting to the following information: $T_{melting}$ = 2,348 K, $\Delta H_{melting}$ =

Table 1 The data were used for liquid Fe phase adjustable parameters optimization

Parameter	Value	Temperature, K	Reference	Calculated value
Melting point, K	1811	1811	[1991Din], [1986Sok]	1811
	1809	1809	[1982Kub]	
Enthalpy of melting, J mol^{-1}	13,800	1811	[1991Din], [1986Sok]	13,806
Heat capacity, J mol^{-1}K^{-1}	45.99	1811	[1991Din]	44.41
	45.99	1900	[1991Din]	45.42
	45.99	2000	[1991Din]	46.46
	41.90	1803–1900	[1979Fin]	44.40–45.42
	44.27	1900	[1963Hul]	45.42
	44.44	2000	[1963Hul]	46.46

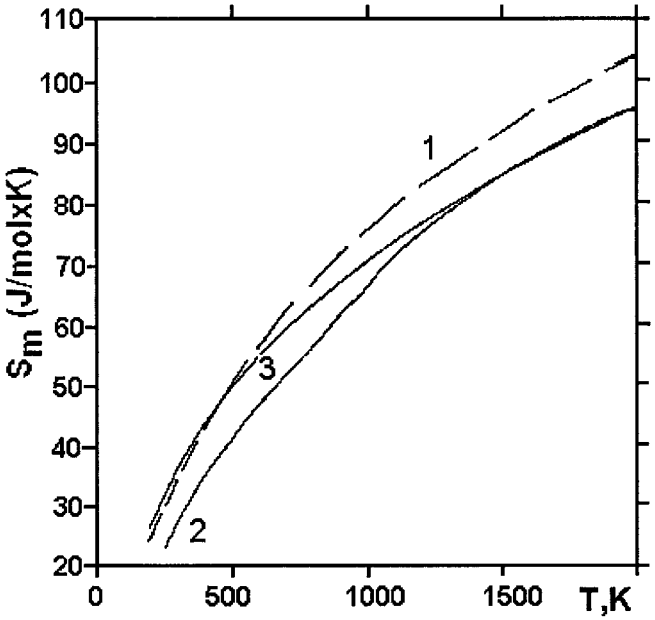

Fig. 1 Molar entropy S_m of pure iron vs temperature T for 1—liquid, 2—bcc, and 3—fcc

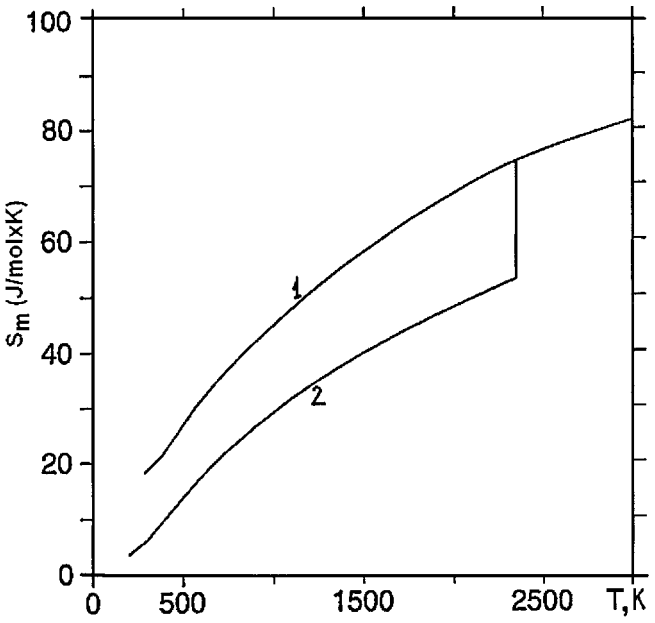

Fig. 2 Molar entropy S_m of pure boron vs temperature T for 1—liquid, and 2—β

50,200 J mol^{-1}, and c_p^{liq} (T_m) = 31.4 J mol^{-1} K^{-1} [1991Din]. The following parameters were obtained: A = 47,528.9 + H_B^{SER} J mol^{-1}, B = 0.0019 J mol^{-1} K^{-2}, D = – 1.91 J mol^{-1} K^{-1}.

The entropies of liquid and solid phases are shown in Fig. 2.

3.3 New Description of Liquid Fe-B

In accordance with Ågren *et al.* [Agr1995], we have chosen to expand the two-state model by applying Eq 1 also for the alloy and expanding ${}^0G_m^{lso}$ and ΔG_d as functions of composition as in the usual regular solution formalism; *i.e.*,

$$ {}^oG_m^{sol} = x_{Fe}^L\ {}^oG_{Fe}^{sol} + x_B^L\ {}^oG_B^{sol} + x_{Fe}^L\ x_B^L\ L_{FeB}^{sol} \quad \text{(Eq 5)} $$

$$ \Delta G_d = x_{Fe}^L\ \Delta G_d^{Fe} + x_B^L\ \Delta G_d^B + x_{Fe}^L\ x_B^L\ \Delta G_d^{FeB} \quad \text{(Eq 6)} $$

Higher order terms as well as temperature dependencies are easily included whenever experimental data indicate a more complex behavior.

The binary phase diagram was first calculated using Thermo-Calc and the SGTE solution database [1985Sun, 1997Sun] with the new descriptions of liquid B and Fe instead of the ordinary ones and using $\Delta G_d^{FeB} = 0$. The parameter L_{FeB}^{sol}, representing the interaction between Fe and B, was simply taken as the normal regular solution parameter of the liquid from the SGTE database, in the present case, a second-order Redlich-Kister polynomial. In Table 2, experimental and calculated invariant points of the phase diagram are compared. As can be seen, the agreement between experimental and calculated values is very good. Figures 3 and 4 show some calculated results for an Fe-15 at.% B alloy. Figure 3(a) depicts the calculated entropy and (b) the Gibbs energy as functions of temperature, and Fig. 4(a) shows the calculated enthalpy and (b) the heat capacity as functions of temperature.

After these preliminary calculations, the calorimetric data obtained from metallic glasses were considered. The general behavior of thermograms of amorphous metallic materials, prepared by rapid quench of the melt, is observed in detail in [1995Bus]. During heating, the heat capacity c_p of metallic glasses behaves as follows. At low temperatures, the heat capacity is quite similar to the heat capacity of a crystalline alloy of the same composition. In the glass transition range, or rather during melting of the glass, a drastic increase in heat capacity is observed. This increase is displaced toward higher temperatures at higher heating rates. After the increase, the heat capacity levels off at a level that does not depend on the heating rate but on temperature only, indicating that the amorphous phase has relaxed to a state of internal equilibrium. The

Table 2 Special points of the Fe-B system (reaction with liquid)

Reaction	Temperature, K Composition, at. %	Reference	Calculated value, *K*
(δFe) ↔ (γFe) + L	1665 ± 10	[1990Mas]	1665
L ↔ (γFe) + FeB_2	1447 ± 30, ≈17	[1990Mas]	1443, ≈17
	1450	[1982Kub]	
	1422	[1958Han]	
L + FeB ↔ FeB_2	1662 ± 20, ≈32.5	[1990Mas]	1683, ≈32.5
	1680	[1982Kub]	
	1662	[1958Han]	
L ↔ FeB	1923, ≈50	[1990Mas]	1900, ≈50
	1863	[1982Kub]	
	≈1823	[1958Han]	
L ↔ FeB + (βB)	1823 ± 10, ≈64	[1990Mas]	1798, ≈64
	1770	[1982Kub]	
	1701	1958Han]	

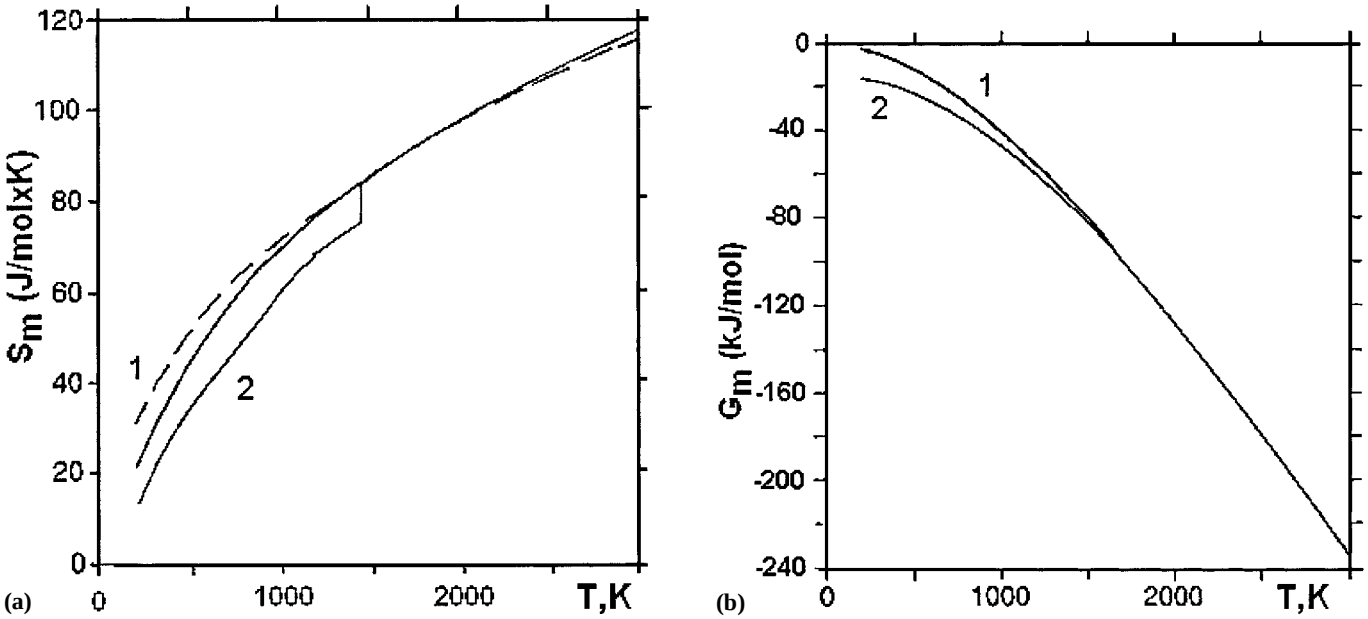

Fig. 3 Calculated temperature dependencies of the $Fe_{85}B_{15}$ alloy thermodynamic functions. 1—liquid state, and 2—thermodynamic stable state. **(a)** Molar entropy S_m. **(b)** Molar Gibbs energy G_m. The dashed line shows the calculated entropy for the supercooled liquid obtained from the SGTE database.

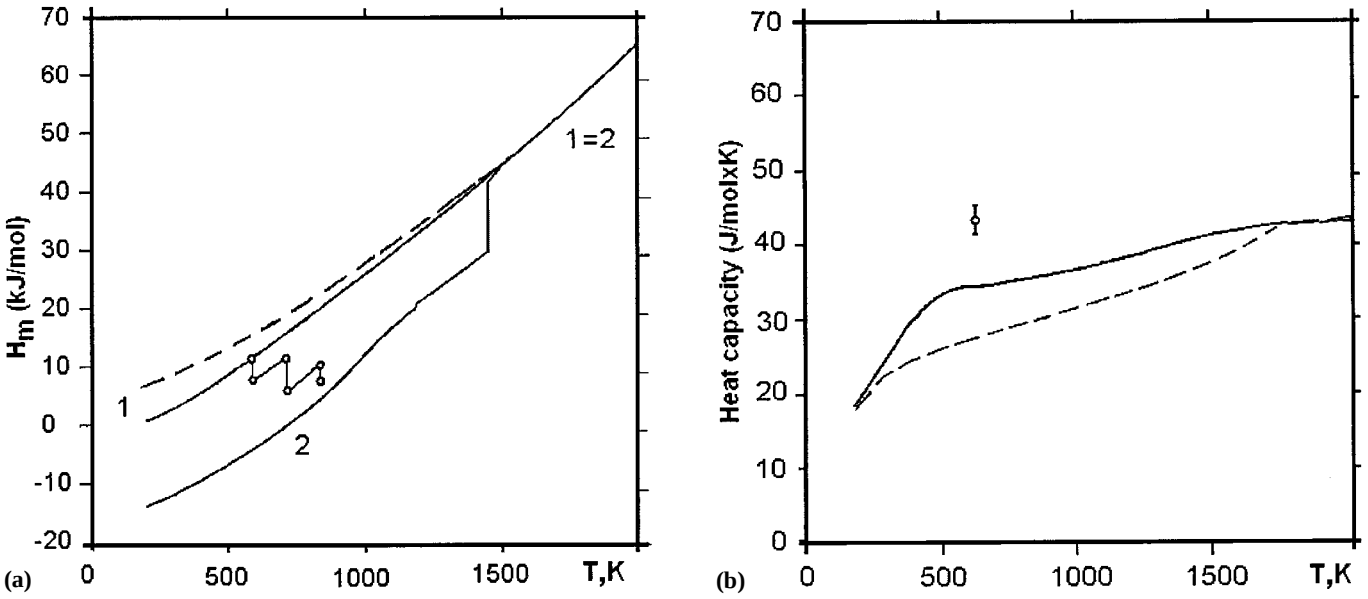

Fig. 4 Calculated temperature dependencies of the $Fe_{85}B_{15}$ alloy thermodynamic functions. 1—liquid state, and 2—thermodynamic stable state. **(a)** Molar enthalpy H_m. The dotted curve is obtained from the DSC experiment. **(b)** Heat capacity of the liquid. The symbol denotes the experimental data. The dashed line is calculated from the SGTE solution database.

most important features of this behavior have been observed in detail [1986Maz, 1991Tol]. Here, we shall only emphasize that at the high-temperature part of the glass transition range, immediately before onset of crystallization, the heat capacity should be close to the heat capacity of the supercooled metastable liquid. By measuring the heat capacity of a metallic glass for various heating rates, it is thus possible to evaluate the heat capacity of the highly supercooled liquid as a function of temperature.

Above the glass transition, there is a strong exothermal effect due to crystallization. It should be noticed that the heat of crystallization is usually more than one order of magnitude larger than the endothermal heat effect associated with relaxation from glass to metastable liquid, see [1995Bus]. Evidently,

the crystallization heat of metallic glasses is an important piece of information when determining the thermodynamic properties of the supercooled liquid. It represents the enthalpy difference between the supercooled and the crystalline state, which is bcc-Fe + Fe_2B for the $Fe_{85}B_{15}$ alloy if the most stable structure forms.

From the DSC measurements, we evaluate for the $Fe_{85}B_{15}$ alloy

$$c_p^{liq}(700\,\mathrm{K}) = 40\ \mathrm{J\,mol^{-1}\,K^{-1}}$$

For the full heat effect of supercooled liquid stable crystal condition, we evaluate

$$\Delta H_{cr} = 10,000\ \mathrm{J\,mol^{-1}}$$

Figure 4(a) shows the experimental DSC results (dotted line) obtained by integrating the experimental c_p curve over the phase transformations region. The upper solid line is calculated from the new description and the upper dashed line from the SGTE description. The lower solid line represents the equilibrium mixture bcc-Fe + Fe_2B. In Fig. 4(b), the solid line is calculated from the new description and the dashed line from the SGTE description. The symbol denotes the experimental c_p^{liq} at 700 K.

4. Discussion

The thermodynamic behavior of the pure elements has been discussed before [1988Agr, 1995Agr] and will not be discussed further here. We shall only conclude that the new description of the pure elements in their liquid states did not affect the calculated phase diagram very much; *i.e.*, the description obtained in the present work may be used as well as the old description for the purpose of calculating the phase diagram. However, if the purpose is rather to obtain a reasonable heat capacity or crystallization heat at large undercooling, the present description yields a much better prediction than the SGTE description despite the fact that the new method is really only a different way of extrapolating the same experimental data as were used in the current SGTE description.

The general thermodynamic features of undercooled liquids have been recognized for a long time. As already mentioned, the liquid has a higher heat capacity than the corresponding crystalline structure upon cooling; *i.e.*, upon cooling, the liquid has a more rapid decrease in entropy and enthalpy than the crystalline structure. If such behavior continues to very low temperatures, there must be a temperature T_s below which the entropy of the liquid becomes lower than the entropy of the stable crystalline state. Kauzmann [1948Kau] was first to describe this situation and regarded it as an unphysical prediction, which could not occur in nature. He also concluded that it would never occur in real liquids, because below the glass transition, both crystal and glass have the same heat capacity and thus the entropy changes with the same rate. Therefore, he concluded that the isentropic temperature T_S must be a lower limit for the glass transition. Theoretical investigations of the vitreous and liquid state (see, for example, [1960Gib, 1976Gor]) have given some further insights into these phenomena, but experimental studies are still quite sparse [1982Gon].

The present investigation of that phenomenon has shown that the enthalpy and entropy differences between equilibrium crystalline state and the liquid state are not as large as predicted from the SGTE database (see Fig. 4a and 3b). However, in the present analysis, there is no isentropic temperature T_S where the entropy difference vanishes. In fact, as can be seen from Fig. 3(b), it is quite large even below room temperature. We may further notice that there is a discrepancy between the measured and calculated heat effect due to crystallization. The calculated enthalpy curve for the equilibrium crystalline phases has a change in slope around 1000 K due to the magnetic transition of the bcc-Fe at the Curie temperature. It is interesting to notice that if it had not been for the magnetic transition upon cooling, there would have been an almost perfect agreement between experiments and calculations. The heat capacity of bcc-Fe becomes very large around the Curie temperature, $c_p^{bcc} > 50\ \mathrm{J\,mol^{-1}\,K}$, and is larger than the heat capacity of the liquid at the same temperatures. Therefore, the entropy and enthalpy differences between the stable crystalline bcc-Fe + Fe_2B state and the liquid state increase upon cooling in the range around 1000 K. On the other hand, if there was also a magnetic transition in the undercooled liquid, having roughly the same heat effect as the transition in bcc-Fe, then we may expect an agreement between calculations and experiments.

These observations thus suggest that the glassy metal would exhibit a magnetic transition similar to the one in bcc-Fe but at a much lower temperature. Such a transition has actually been reported by Kisdi-Koszó *et al.* [1997Kis] for the present alloy at 530 K. If we assume that this magnetic transition has the same contribution to the heat capacity as the one in bcc-Fe, except that the Curie temperature is 530 K, we may easily calculate its effect on the thermodynamic properties. The result is shown in Fig. 5(a) to (c). Figure 5(a) is identical to 4(b), except that the upper curve, representing the new evaluation including a magnetic contribution, has been added. As can be seen, there is now a very good agreement between the experimental heat capacity and the calculations. Figure 5(b) is the same as 4(a), but the curve, marked 3, has been calculated from the new evaluation with the magnetic contribution added. The agreement between experiments and calculations is now excellent.

5. Summary

In the present paper, we have investigated experimentally a glassy Fe-15 at.% B alloy and analyzed the results in terms of the two-level model for undercooled liquids. This model allows reasonable extrapolation of the thermodynamic properties of liquid Fe-B alloys to large undercooling. The new model yields practically the same phase diagram as the SGTE database but gives different results for quantities such as the heat capacity, entropy, and crystallization heat at low temperatures. The calculations have been compared with the experimental data, and it is found that an excellent agreement between calculations and experiments is obtained if the effect of the reported magnetic transition at 530 K is taken into account.

The present description of supercooled liquid iron-boron alloys should thus be regarded as quite satisfactory and superior

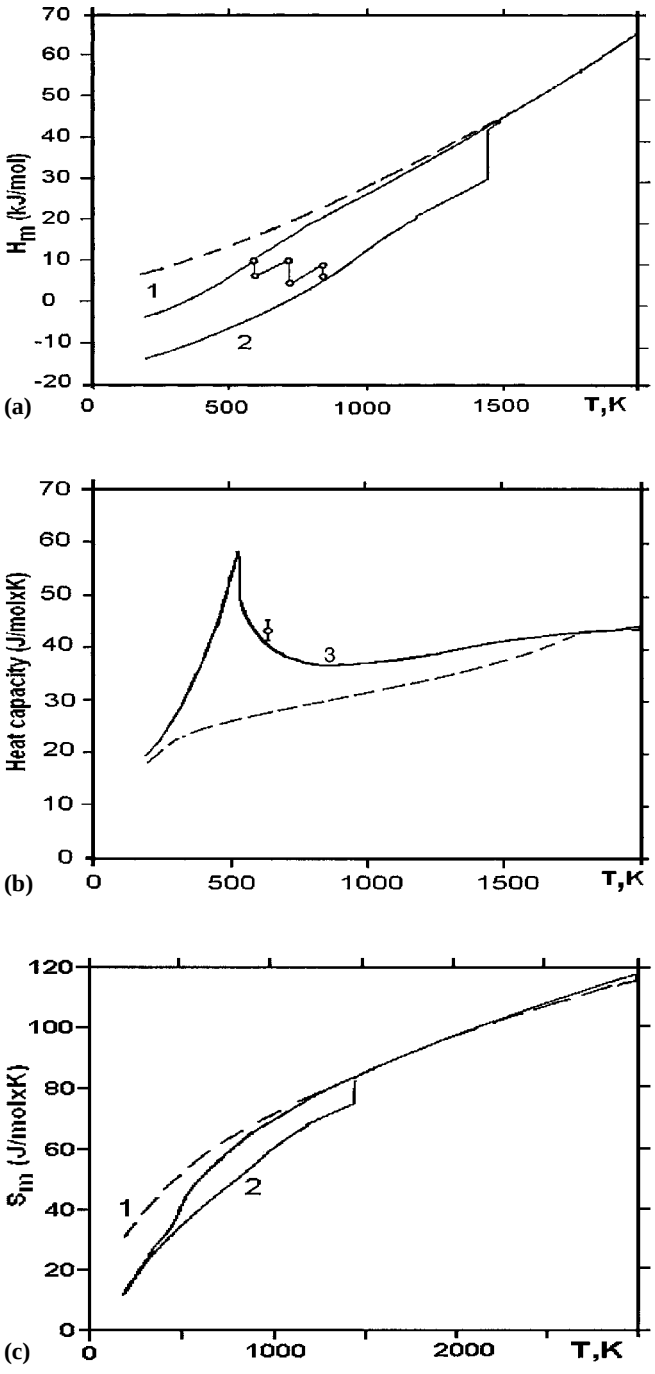

Fig. 5 Calculated temperature dependencies of the $Fe_{85}B_{15}$ alloy thermodynamic functions taking the magnetic transition in the amorphous phase into account. **(a)** Molar enthalpy H_m. **(b)** Heat capacity of the liquid. **(c)** Molar entropy S_m. See also Fig. 3 and 4.

to the one in the SGTE database. One should now apply the two-state model also to other binary systems, *e.g.* Fe - Si, and then eventually to multicomponent glassy metals.

Acknowledgments

The authors would like to express their sincere gratitude to Drs. A. Borgenstam and M. Selleby at the Royal Institute of Technology (KTH) in Stockholm, for their great assistance with the calculations. The Swedish Institute is gratefully acknowledged for a grant allowing Dr. Tolochko to visit KTH.

References

1948Kau: W. Kauzmann: *Chem. Rev.*, 1948, vol. 43 (1), pp. 219-56.
1958Han: M. Hansen and K. Anderko: *Constitution of Binary Alloys*, McGraw-Hill Book Company, New York, NY, 1958, p. 250.
1960Gib: J.H. Gibbs: In *Modern Aspects of the Vitreous State*, J.D. Machenzie, Butterworth, London, 1960, pp. 152-87.
1963Hul: R. Hultgren, R.L. Orr, P.D. Anderson, and K.K. Kelley: *Selected Values of Thermodynamic Properties of Metals and Alloys*, University of California, Berkeley, CA, 1963, pp. 103-12.
1976Gor: J.M. Gordon, J.H. Gibbs, and P.D. Flemming: *J. Chem. Phys.*, vol. 65 (7), pp. 2771-78, 1976.
1979Fin: H.A. Fine and G.H. Geiger: *Handbook on Material and Energy Balance Calculations in Metallurgical Processes*, TMS-AIME, Warrendale, PA, 1979, p. 431.
1982Gon: N.O. Gonchykova: Fiz. Khim. Stekla (Sov. J. Glass Phys. Chem.), 1982, vol. 8 (4), pp. 429-34 (in Russian).
1982Kub: O. Kubaschewski: *Iron-Binary Phase Diagrams*, Springer-Verlag, Berlin, and Verlag Stahliisen mbH, Dusseldorf, 1982, p. 16.
1985Lel: Shrikant Lele, K.S. Dubey, and P. Ramachandrarao: *Curr. Sci.*, vol. 54 (19), pp. 994-95, 1985.
1985Sun: B. Sundman, B. Jansson, and J.-O. Andersson: *CALPHAD*, Vol. 9 (1985) p. 153
1986Maz: O.V. Mazurin: *Steklovanie (Glass Transition)*, Nayka, Leningrad, 1986 (in Russian)
1986Sok: E.M. Sokolovskaya and L.S. Gysei: *Metallikhimiya (Metal Chemistry)*, Moscow University, Moscow, 1986 (in Russian).
1988Agr: J. Ågren: *Phys. Chem. Liq.*, 1988, vol. 18, pp. 123-39, 1991.
1990Mas: *Binary Alloy Phase Diagrams*, T.B. Massalski, ed., ASM INTERNATIONAL, Materials Park, OH, 1990, pp. 482-83.
1991Din: A.T. Dinsdale: *CALPHAD*, vol. 15 (4), pp. 317-425.
1991Tol: O.V. Tolochko and N.O. Gonchykova: *Fiz. Khim. Stekla (Sov. J. Glass Phys. Chem.)*, 1991, vol. 17 (2), pp. 214-18 (in Russian).
1995Agr: J. Ågren, B. Cheynet, M.T. Clavaguera-Mora, J. Hertz, F. Sommer, and U. Kattner: CALPHAD, vol. 19 (4), pp. 449-80, 1995.
1995Bus: R. Busch, Y.J. Kim, and W.L. Johnson: *J. Appl. Phys.*, vol. 77 (8), pp. 4039-43, 1995.
1997Kis: É. Kisidi-Koszó, L.F. Kiss, L.K. Varga, and P. Kamasa: Mater. Sci. Eng., 1997, vols. A226-A228, pp. 689-92.
1997Sun: B. Sundman: *Thermo-Calc User's Guide*, Royal Institute of Technology, Stockholm, 1997.